# Velocity independent seismic imaging

*Richard Ottolini*

Normally, to image seismic data, one needs to know the velocity at every sub-surface location. However it is possible to image seismic data by knowing the time dip(s) of the seismic data at every point on the recorded seismic data. The advantage of this second scheme is that time dips, in contrast to velocities, can be measured automatically without picking. The algorithm in this paper is to decompose the seismic data into sections of constant time dip, apply a velocity independent imaging operation to each dip section, and finally recompose the dip sections into an image. This method applies where there are laterally redundant reflections from the same sub-surface point in the form of a hyperbola. This includes zero offset section diffractions, stacking, and migration before stack in depth variable velocity media.

## Velocity independent hyperbola summation

The velocity parameter, $v$, in the equation of a hyperbola for two-way travel time

$$t_0 = \sqrt{t^2 - \frac{4\Delta x^2}{v^2}} \tag{1}$$

may be replaced by the time dip, $p$, of the seismic data. The time dip is computed from equation (1) by

$$p = \frac{\partial t}{\partial x} = \frac{4\Delta x}{vt^2}. \tag{2}$$

Then the hyperbola equation becomes

$$t_0 = \sqrt{t^2 - p\Delta x t}. \tag{3}$$

Equation (3) is used for hyperbola summation in this paper. Given the seismic data decomposed into sections of constant dip $(p, x, t)$, equation (3) defines an *all-velocity* curve,

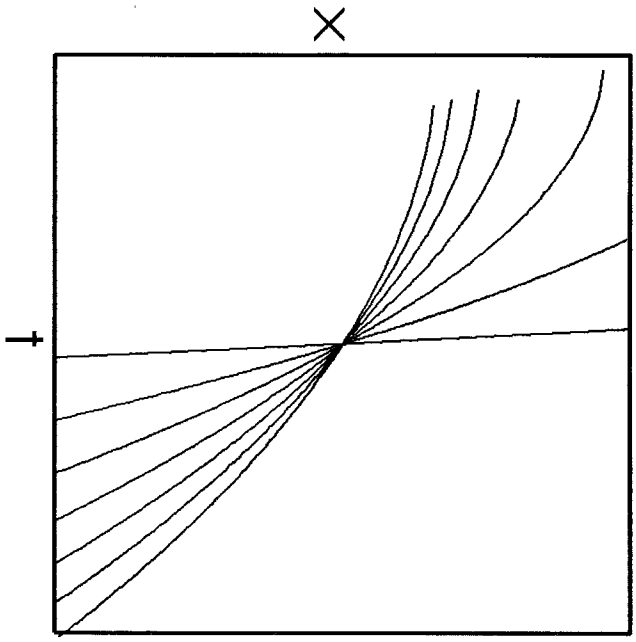

FIG. 1. All-velocity curves emanating from the same $(x, t)$ point, except for different dips.

that is $(t_0, \Delta x)$ as a function of known $(p, x, t)$. Figure 1 graphs all-velocity curves for various dip slopes at the same $(x, t)$ point.

If there are redundant reflections from the same sub-surface reflection point $(x, t_0)$, then the all-velocity curves generated from the redundant reflections will intersect at that sub-surface point. Figure 2 illustrates this concept graphically using a hyperbola. This intersection means that equation (3) instantiated at two or more $(p, x, t)$ points can be solved for $x$, $t_0$, and $v$.

If there are no redundant reflections from the same sub-surface point, then the all-velocity curves will not intersect or the intersections will be random. Take for example the dipping line segment in a constant velocity medium as shown in Figure 3. The all-velocity curves do not intersect in the sub-surface and we cannot solve for the image point or imaging velocity in this case. This is because the various reflection points along the line segment come from different sub-surface reflectors. A mathematical proof of non-intersection for straight line segments is given in the appendix.

## Seismic data dip decomposition

A discussion of dip decomposition of seismic data into $(p, x, t)$ space is given by Ottolini

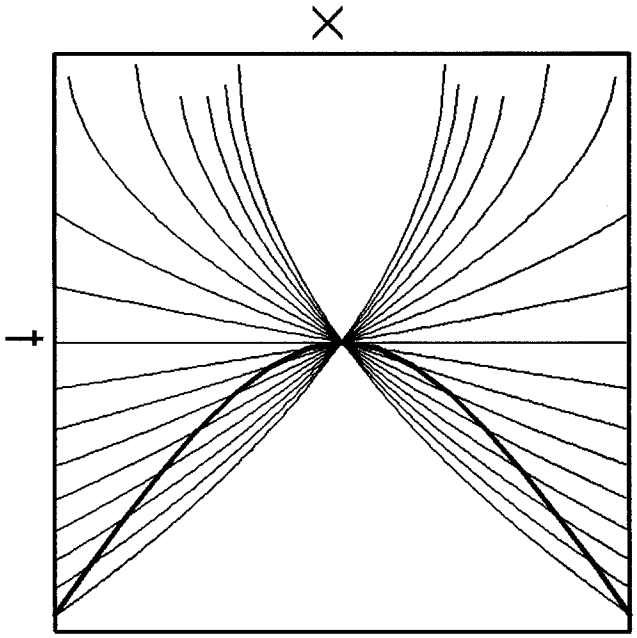

FIG. 2. All-velocity curves emanating from points along the side of the hyperbola intersect at the apex of the hyperbola.

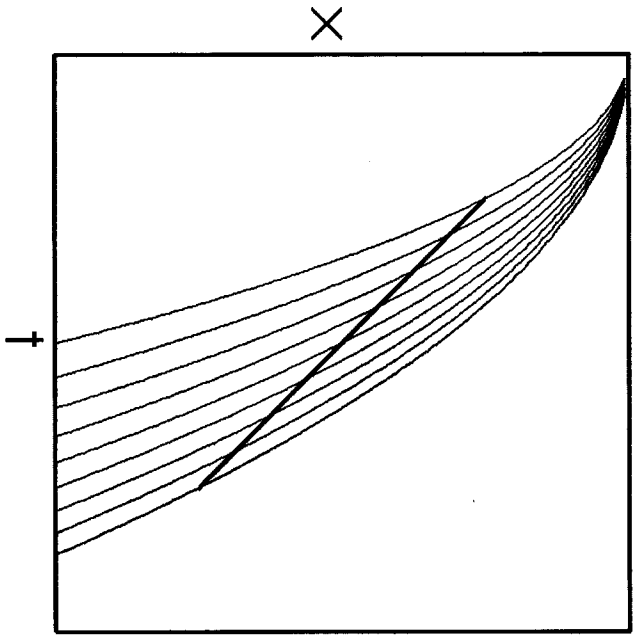

FIG. 3. The all-velocity curves from a straight line segment do not intersect.

elsewhere in this SEP report. An efficient method of computing local slant stacks similar to the dip mix of Robinson and Robbins (1978) is used.

Preliminary field data experiments (not included in this paper) indicate that the dip decomposition is a crucial stage in the imaging algorithm. It is best to know a precise $p$ spectra for every $(x,t)$ location. However, because of the lateral mixing within a Fresnel zone and band-limited frequency content of the seismic data, there is an uncertainty range of $p$ and location.

## Migration after stack

Migration after stack is the weakest implementation of this scheme because there are redundant reflections only as diffractions. The most obvious implementation of equation (3) to compute the migration all-velocity curves is a diffraction summation implementation. But this is slow when repeated for every midpoint and dip. Amplitude corrections in the form of a cosine dip correction and vertical derivation are required in diffraction summation migration (Schneider, 1978). The cosine correction is simply

$$\cos\theta = \sqrt{1 - \frac{p^2 v^2}{4}} = \sqrt{1 - \frac{p\Delta x}{t}}. \tag{4}$$

A more efficient f-k implementation of equation (3) can be derived. First one constructs the dispersion relation

$$\omega_0 = \sqrt{\frac{k\omega}{p} - \frac{4k^2}{p^2}} \tag{5}$$

by assuming that equation (3) is a characteristic curve of geometrical optics. The mathematics is done in the appendix. (Note that these are the Fourier variables of a dip decomposed section rather than the original data. All same dip information in the original data lies along a single radial line in the Fourier transformed original data.) The dispersion relation gives the Fourier domain coordinate transformation of the dip decomposed data

$$u(k,\omega_0) = \frac{k}{2p\omega} u(k, \omega = \left[\frac{p\omega_0^2}{k} + \frac{4k}{p}\right]) \tag{6}$$

which is the heart of the f-k method.

A synthetic f-k migration is shown in Figure 4. The wider the $p$ range, the tighter the focus. The greater the number of $p$ values, the greater the increase of signal over numerical noise. The secondary focii are caused by wrap-around parts of all-velocity curves intersecting.

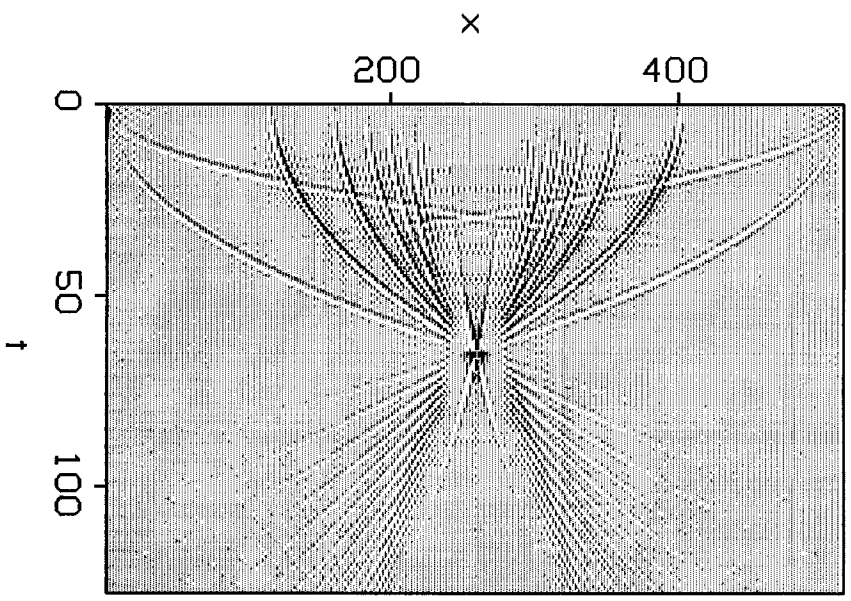


FIG. 4. Wave equation velocity independent migration using a f-k alogorithm. The hyperbola velocity was .3 .

## Stacking before migration

Velocity independent stacking is similar to velocity independent migration, but with a few important differences.

- All reflections are more or less laterally redundant. So all reflections to focus to an image.
- We know that the focus will be at zero offset (assuming no lateral velocity variations). Therefore we only need to compute equation (3) for the zero offset $\Delta x$. This means that equation (3) is better implemented as a moveout rather than a wave equation as in the migration case. A processing sequence would be

  (1) Dip decompose a CDP gather.

  (2) Apply all-velocity moveout (AVMO) to each dip gather to obtain a zero offset trace.

  (3) Recompose the zero offset trace by summing all the dips together or some other means
- Since dipping events on a CDP gather are hyperbolas to a more or less degree, velocity independent stacking will work on dipping events, including events of different dips intersecting at the same midpoint. However, the image of the dipping event won't be entirely accurate. The dipping event CDP hyperbola actually arises from different sub-surface reflection points. Therefore, the overall dipping event will be smeared out

into more CDP's than it should be.

## Migration before stack

Velocity independent migration before stack solves problems of velocity independent migration after stack and velocity independent stacking before migration. First, it will image line segments. Second, it will handle dipping events correctly. The major drawback is operational. If the seismic data is decomposed into $N$ dip components in the midpoint direction and $M$ dip components in the offset direction, then each unstacked data trace much be decomposed into $N \times M$ dip traces. This is considerably more expensive than stacking before migration and migration after stack. However, there may be some hybrid of conventional methods and velocity independent methods which have a lower cost. Most of the benefits arise from the stacking side of the algorithm, so the migration half might be done in a more conventional manner.

The derivation of an all-velocity *surface* follows that of the all-velocity curve. We begin with the travel time for a source and receiver separated by offset $2h$.

$$t = \frac{1}{v}\left[\sqrt{z^2 + (\Delta x + h)^2} + \sqrt{z^2 + (\Delta x - h)^2}\right]. \tag{7}$$

This travel time surface has the shape of a pyramid where $z = vt_0/2$ is the depth to the apex of the pyramid. Solving equation (7) for the apex of the pyramid $t_0$ as a function of midpoint separation $\Delta x$, half-offset $h$, travel time $t$, and velocity $v$ gives

$$t_0 = \sqrt{t^2 - \frac{4\Delta x^2}{v^2} - \frac{4h^2}{v^2} + \frac{16\Delta x^2 h^2}{v^4 t^2}}. \tag{8}$$

Following equation (3) we may define the midpoint and offset dips to be

$$p_x = \frac{4\Delta x}{v^2 t} \qquad p_h = \frac{4h}{v^2 t}. \tag{9}$$

With these definitions equation (8) becomes the all-velocity surface

$$t_0 = \sqrt{t^2 - p_x \Delta x t - p_h h t + p_x p_h \Delta x h t^2}. \tag{10}$$

Equation (10) is the migration before stack equivalent of equation (3). In the zero offset cases, $\Delta x = 0$ or $h = 0$, equation (10) reduces to equation (3). I have not been able to construct and test a dispersion relation and f-k algorithm for equation (10), but a good guess is presented in the appendix.

## Appendix A: All-velocity curve non-intersection proof

This appendix proves that the all-velocity curves emanating from a straight segment intersect at $t_0 = 0$. Since the obliquity weight function, equation (4), becomes zero at $t_0$, then this focusing will not be a problem.

All-velocity curves from segment points $(t_1, x_1)$ and $(t_2, x_2)$ will intersect when their $(t_0, \Delta x)$ are the same. Define point $(t_2, x_2)$ to be $\Delta y$ lateral distance from point $(t_1, x_1)$ on the same line segment. Then

$$t_2 = t_1 + p\Delta y \qquad \Delta x_2 = \Delta x_1 + \Delta y. \tag{A-1}$$

If the intersection point $(t_0, \Delta x)$ is the same for all-velocity curves emanating from each segment point, then from equation (3)

$$\sqrt{t_1^2 - p\Delta x_1 t_1} = \sqrt{t_2^2 - p\Delta x_2 t_2} = \sqrt{(t_1 + p\Delta y)^2 - p(\Delta x_1 + \Delta y)(t_1 + p\Delta y)}. \tag{A-2}$$

Equation (A-2) solves for all $\Delta y$, $\Delta x_1 = \frac{t_1}{p}$, and $t_0 = 0$, thereby proving that the there is no intersection point below the surface.

## Appendix B: Dispersion relation construction

Given the characteristic give curve

$$t_0 = \sqrt{t^2 - p\Delta x t} \tag{B-1}$$

this appendix will construct a dispersion relation which generates it. I was not able to find a systematic method of obtaining dispersion relations from characteristic curves. Also, the answer is not unique. An answer was eventually found by working both forwards from the characteristic curve and backwards from a general template of dispersion relations, and testing the result in a computer program.

We will assume a dispersion relation $\phi$ which can be used in a continuation operator $\exp(i\phi t_0)$. This continuation operator when convolved with an impulse response, $\delta(x,t)$, numerically constructs the characteristic curve

$$u(x, t_0, \omega) = \int_{-\infty}^{\infty} \int_{-\infty}^{\infty} \mathrm{FFT}\left[\delta(x,t)\right] \exp(i\phi t_0)\, dk d\omega \, \exp(ikx - i\omega t). \tag{B-2}$$

Next, by the method of stationary phase we derive a differential equation which the dispersion relation must satisfy. The method of stationary phase says that most of the

above integral's contribution to the result will occur at a stationary point of the exponential phase

$$\psi = \phi t_0 + kx - \omega t. \qquad (B-3)$$

The stationary points are determined by

$$\frac{\partial \psi}{\partial k} = 0; \qquad \frac{\partial \psi}{\partial \omega} = 0; \qquad (B-4ab)$$

$$\frac{\partial \phi}{\partial k} t_0 + x = 0; \qquad \frac{\partial \phi}{\partial \omega} t_0 - t = 0. \qquad (B-4cd)$$

Plugging equations (B-4cd) into the characteristic curve (B-1) gives an eikonal differential equation which the dispersion relation must satisfy

$$\phi_\omega^2 + p\,\phi_\omega \phi_k = 1. \qquad (B-5)$$

There are an unlimited number of solutions to equation (B-5). By analogy to the general two dimensional wave equation dispersion relation, we will assume a solution that is quadratic in wavenumber. We try a solution of the form $\phi = \sqrt{\varphi}$ where

$$\varphi = ak^2 + b\omega^2 + ck\omega + dk + e\omega + f. \qquad (B-6)$$

Making this $\phi$ substitution changes equation (B-5) to

$$\varphi_\omega^2 + p\,\varphi_\omega \varphi_k = 4\varphi. \qquad (B-7)$$

where

$$\varphi_\omega = 2b\omega + ck + e; \qquad \varphi_k = 2ak + c\omega + d. \qquad (B-8ab)$$

Equating terms of the same power on each side of equation (B-8) gives the relations

$$a = 4c^2 + 2acp; \qquad (B-9a)$$

$$b = 2b^2 + 2bcp; \qquad (B-9b)$$

$$c = 4bc + 4abp + c^2 p; \qquad (B-9c)$$

$$d = 2ec + dp + 2aep; \qquad (B-9d)$$

$$e = 2be + cep + 2bdp; \qquad (B-9e)$$

$$f = e^2 + edp. \qquad (B-9f)$$

There is no unique answer to the system of equations (9a-f). Fortunately, the simplest consistent solution gives a workable answer. That solution is to let $b = 0$, $d = 0$, $e = 0$, and $f = 0$. Then $a = -4/p^2$ and $c = 1/p$. Finally, we obtain the answer

$$\phi = \omega_0 = \sqrt{\frac{k\omega}{p} - \frac{4k^2}{p^2}}. \qquad (B-10)$$

The migration before stack dispersion relation can be constucted in a similar way. The eikonal equivalent for equation (10) is

$$(\phi_\omega + p_x \phi_{k_x})(\phi_\omega + p_h \phi_{k_h}) = 1. \qquad (B-11)$$

I have not yet been able to obtain a quadratic solution in wavenumber for this equation. A trial solution of the form

$$\phi = \sqrt{ak_x^2 + bk_h^2 + c\omega^2 + dk_x k_h + ek_x\omega + fk_h\omega} \qquad (B-12)$$

leads to a not easily solved set of coefficient relations.

$$a = e^2 + 2aep_x + dep_h + 2adp_x p_h; \qquad (B-13a)$$

$$b = f^2 + dfp_x + 2bfp_h + 2bdp_x p_h; \qquad (B-13b)$$

$$c = 4c^2 + 2cep_x + 2cfp_h + efp_x p_h; \qquad (B-13c)$$

$$d = 2ef + 2afp_x + edp_x + 2bep_h + dfp_h + 4abp_x p_h + d^2 p_x p_h; \qquad (B-13d)$$

$$e = 4ce + e^2 p_x + 4acp_x + 2cdp_h + efp_h + 2afp_x p_h + dep_x p_h; \qquad (B-13e)$$

$$f = 4cf + efp_x + 2cdp_x + 4cbp_h + f^2 p_h + dfp_x p_h + 2bep_x p_h. \qquad (B-13f)$$

My next best guess is a solution of the form

$$\phi = \sqrt{\left(\frac{k_x}{p_x} + \frac{k_h}{p_h}\right)\omega - 4\left(\frac{k_x}{p_x} + \frac{k_h}{p_h}\right)^2} + \sqrt{\left(\frac{k_x}{p_x} + \frac{k_h}{p_h}\right)\omega - 4\left(\frac{k_x}{p_x} - \frac{k_h}{p_h}\right)^2}. \qquad (B-14)$$

based on symmetry, equation (B-10), and analogies with derivation of the double square root dispersion relation. However, it takes a lot of algebra to prove whether equation (B-14) satisfies equation (B-11).

## REFERENCES

Robinson, J.C. and Robbins, T.R., 1978, Dip-domain migration of two-dimensional seismic profiles: Geophysics, v. 43, p. 77–93

Schneider, W.A., 1978, Integral formulation for migration in two and three dimensions: Geophysics, v. 43, p. 49–76

**"But YES the hippopotamus!"**

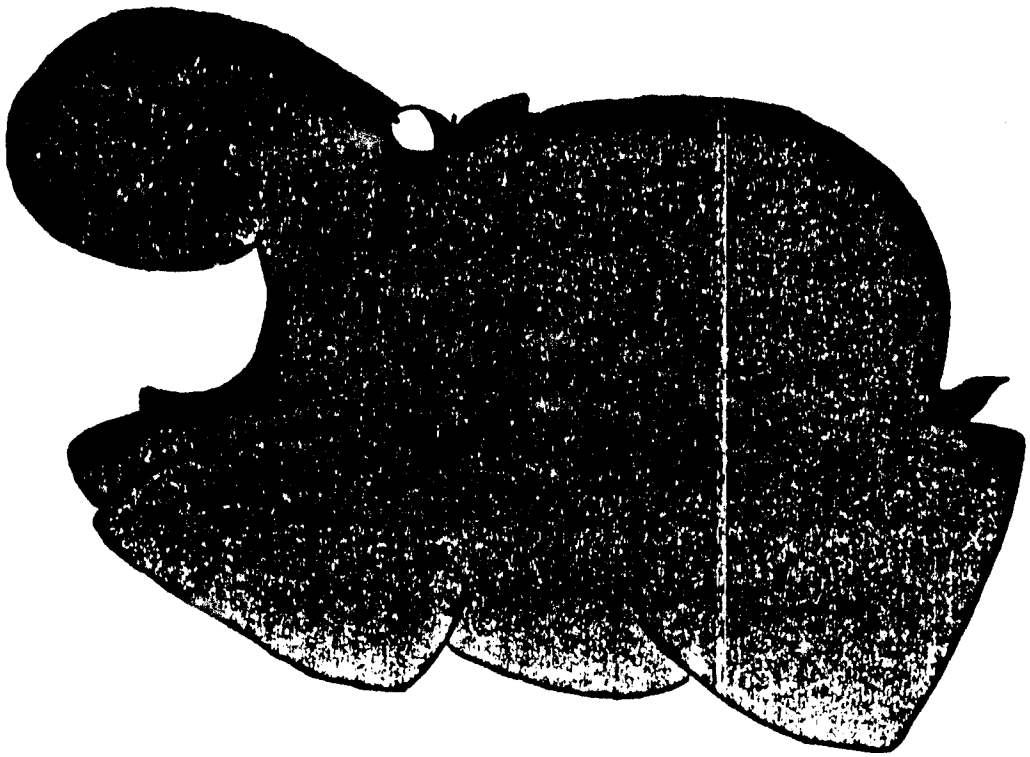

**But not the armadillo.**